

Hepatitis B virus (HBV) capsid recycling and de novo secondary infection events maintain stable cccDNA levels

Chunkyu Ko¹, Anindita Chakraborty^{1,2}, Wen-Min Chou¹, Julia Hasreiter¹, Jochen M. Wettengel¹, Daniela Stadler¹, Romina Bester¹, Theresa Asen¹, Ke Zhang¹, Karin Wisskirchen¹, Jane A. McKeating^{2,3}, Wang-Shick Ryu⁴, and Ulrike Protzer^{1,2,5}

¹Institute of Virology, Technische Universität München / Helmholtz Zentrum München, Munich, Germany

²Technische Universität München, Institute for Advanced Study, Munich, Germany

³Nuffield Department of Medicine, University of Oxford, Oxford, United Kingdom

⁴Department of Biochemistry, Yonsei University, Seoul, Korea

⁵German Center for Infection Research (DZIF), Munich partner site, Munich, Germany

Corresponding author: Ulrike Protzer (protzer@tum.de)

Institute of Virology, Technische Universität München / Helmholtz Zentrum München, Trogerstrasse 30, 81675 Munich, Germany

Tel: +49 8941406886; Fax: +49 8941406823

Key words: HBV; hepatitis B virus; cccDNA; NTCP; replenishment; reinfection; virus spread; transmission; intracellular recycling; PEG; DMSO

Electronic word count: abstract 255 words, main text 6,310

Number of figures and tables: 6 figures and 1 table

Conflict of interest statement

The authors disclose no conflicts of interest

Financial support statement

The work was supported by the German Research foundation via project 14 in collaborative research center TRR 179. UP and JAM receive funding by the Institute for Advanced Study with the support of the Technical University of Munich via the German Excellence Initiative and EU 7th Framework Program under grant agreement number 291763 and via the EU network Hepcar within Horizon 2020.

Authors contributions

CK, WR, UP designed the study; CK, AC, WC, JH, RB performed the experiments; JMW, DS, TA, KZ, KW provided key materials; CK, AC, JAM, UP wrote and finalized the manuscript.

Abstract

Background & Aims: Several steps of the HBV life-cycle including particle entry, formation and maintenance of covalently closed circular (ccc) DNA, kinetics of gene expression and viral transmission routes remain obscure due to a lack of robust *in vitro* infection models. This study aimed to investigate infection kinetics and cccDNA dynamics during long-term culture.

Methods: We selected a highly permissive HepG2-NTCP-K7 cell clone engineered to express sodium taurocholate co-transporting polypeptide (NTCP) that supports the full HBV life-cycle and characterized its replication kinetics and dynamics over 6 week-infection.

Results: HBV infection kinetics showed a slow infection process. Nuclear cccDNA was only detected 24 hours post-infection and increased until 3 days post infection (dpi). Viral RNAs increased from 3 dpi reaching a plateau at 6 dpi. HBV protein levels followed this kinetics with HBx levels rising first. cccDNA levels modestly increased throughout the 45-day study period with 5 - 12 copies per infected cell. Newly produced relaxed circular (rc) DNA within capsids was reimported into the nucleus and replenished the cccDNA pool. In addition to intracellular capsid recycling, secondary *de novo* infection events resulted in cccDNA formation. Inhibition of rcDNA formation by nucleoside analogue treatment of infected cells enabled us to measure cccDNA dynamics showing a slow decay with a half-life of about 40 days.

Conclusions: After a slow infection process, HBV maintains a stable cccDNA pool by intracellular capsid recycling and via secondary infection. Our results provide

important insights into the dynamics of HBV infection and support the future design and evaluation of new antiviral agents.

Lay summary: Using a highly permissive hepatocellular model system, we demonstrate that HBV has a remarkably slow infection kinetics. Establishment of the episomal transcription template and persistence form, so called cccDNA, but also viral transcription and protein expression is protracted. Once established, HBV maintains a stable pool of cccDNA via intracellular capsid recycling and through infection of naive cells by newly formed virions.

Introduction

Hepatitis B virus (HBV) chronically infects 257 million individuals worldwide and is a major driver of end-stage liver diseases such as cirrhosis and hepatocellular carcinoma [WHO 2017]. The immense death toll of 887,000 individuals/year drives an intensive search for curative treatment approaches. However, a more detailed understanding of infection kinetics and the genesis and maintenance of episomal nuclear DNA pools, so called covalently closed circular (ccc) DNA, is needed to guide the development of an HBV cure.

HBV is a hepatotropic enveloped DNA virus consisting of a 3.2-kb partially double-stranded genome, termed relaxed circular (rc) DNA [1]. Initial interaction with heparansulfate proteoglycans allows virus attachment to the plasma membrane [2, 3] and is critical for subsequent interactions with sodium taurocholate co-transporting

polypeptide (NTCP) as a functional receptor required for HBV infection [4, 5]. Upon interaction with NTCP, the viral particle is internalized and following fusion of the viral and cellular membranes the capsid is released into the cytoplasm and transported to the nucleus. At the nuclear pore, rcDNA is released into the nucleus where it is converted into cccDNA. cccDNA serves as the transcriptional template for pregenomic RNA (pgRNA) and subgenomic RNAs and permits the persistence of HBV infection (summarized in [6]). The pgRNA is packaged together with HBV polymerase into newly formed capsids and reverse transcribed giving rise to progeny rcDNA. Mature, rcDNA-containing capsids are enveloped at the endoplasmic reticulum and secreted via multivesicular bodies [7]. Alternatively, these capsids can traffic back to the nucleus, where they release newly formed rcDNA that can replenish the cccDNA pool [8, 9]. This cycle can be prevented by inhibitors of reverse transcription or by core protein allosteric modulators that have not only been reported to inhibit formation of rcDNA-containing capsids but also to perturb cccDNA biosynthesis (unpublished data and [10]).

An alternative pathway to maintain the cccDNA pool is via secondary infection of naïve cells or pre-infected cells by extracellular virus particles. Enveloped viruses can initiate new infection events via the transfer of extracellular particles to naïve target cells or via direct cell-to-cell contacts [11]. Cell-free spread of extracellular progeny virus allows transition throughout the body to infect distant cells or organs or even a new host. It can be prevented by neutralizing antibodies or entry inhibitors targeting virus-receptor interaction. In contrast, direct cell-to-cell transmission routes enable a virus to evade neutralizing antibodies or complement and are resistant to

entry inhibitors. For hepatitis C virus (HCV) it has been proposed that cell-to-cell spread facilitates immune escape and circumvents rate-limiting steps of the viral life cycle, like attachment and entry [12].

HBV transmission routes that establish and maintain a cccDNA pool are poorly understood, reflecting the paucity of *in vitro* culture systems that support long-term and secondary infection events. Neither the longevity nor the size of the cccDNA established by HBV has been accurately measured [6]. In this study, we developed a highly permissive HepG2 clone stably expressing NTCP, designated HepG2-NTCP-K7, that enabled us to determine the kinetics of the viral life cycle and to study HBV transmission pathways underlying cccDNA persistence. Our studies highlight a slow infection kinetics and a distinct order of expression of viral RNAs and proteins, defined the size of the cccDNA pool and cccDNA half-life and importantly showed modest increases in cccDNA levels over several weeks of cell culture. Furthermore, we demonstrate a role for both capsid recycling and extracellular particle-mediated infection to maintain cccDNA levels.

Materials and Methods

Cell lines

HepG2-NTCP cells were generated using a lentiviral vector encoding human NTCP under the control of a CMV promoter. NTCP cDNA was synthesized by reverse transcription of mRNA from differentiated HepaRG cells. Transduced cells were

selected with blasticidin (30 µg/ml) and best growing single cell clones were screened for their ability to support HBV infection. The clone HepG2-NTCP-K7 was selected for our studies (Supplementary Fig.1). Other cell lines and clones used are detailed in the Supplementary Methods. All cells were maintained in Dulbecco's Modified Eagles Medium (DMEM) supplemented with 10% fetal bovine serum (FBS), 2 mM L-glutamine, penicillin/streptomycin, 1 mM sodium pyruvate and non-essential amino acids (ThermoFisher Scientific, Waltham, MA, USA).

HBV infection

HBV was purified and concentrated from the culture medium of stable HepAD38 producer cells by heparin affinity chromatography followed by sucrose gradient ultracentrifugation. HBV inocula were diluted to 50% FBS/20% sucrose to a final concentration of $2-3 \times 10^{10}$ DNA-containing virus particle (vp)/ml. Unless otherwise indicated, HepG2-NTCP-K7 cells were seeded on collagen-coated plates and pre-differentiated with 2.5% DMSO for 2 days prior to infecting with HBV in the presence of 4% polyethylene glycol (PEG) 6000 for 20-24 hours. The inoculum was removed by extensive washing with PBS and cells were cultured in the presence of 2.5% DMSO.

Real time PCR (qPCR) quantification of HBV genomes

Total cellular DNA was extracted using NucleoSpin Tissue kit (Macherey Nagel). For selective cccDNA PCR, isolated DNA was treated with 5 units of T5 exonuclease (NEB, Frankfurt, Germany) for 30 min in 10 µl reaction volume followed by heat-inactivation at 95°C for 5 min and 4-fold dilution with distilled water [13]. Two different

primer sets were used to detect total intracellular HBV-DNA (HBV1844F: 5'-GTTGCCCCGTTTGTCTCTAATTC-3' and HBV1745R: 5'-GGAGGGATACATAG-AGGTTTCCTTGA-3') and cccDNA (cccDNA92F:5'-GCCTATTGATTGGAAAGTATGT-3' and cccDNA2251R: 5'-AGCTGAGGCGGTATCTA-3') [13]. For HBV-DNA quantification, an external plasmid standard was used. For relative quantification, a dilution series of infected cells was used with the human prion protein (*PRNP*) gene serving as a reference (PRNPF: 5'-TGCTGGGAAGTGCCATGAG-3' and PRNPR: 5'-CGGTGCATGTTTTTCACGATAGTA-3'). To determine cccDNA half-life, cccDNA and intracellular total HBV-DNA levels were normalized by two reference genes encoding *PRNP* and mitochondrial cytochrome c oxidase subunit 3 (*MT-CO3*) [14]. qPCR was performed using LightCycler480 instrument (Roche, Basel, Switzerland)

Imaging HBV core protein expressing cells

HBV-infected cells seeded on 12 mm coverslips were fixed with 4% paraformaldehyde and permeabilized with 0.5% saponin. Cells were then incubated with rabbit anti-core serum (DAKO) followed by Alexa Flour 594-coupled secondary antibody incubation (Invitrogen, Carlsbad, CA, USA). After immunostaining, coverslips were mounted with Fluoromount-G containing DAPI (SouthernBiotech, Birmingham, AL, USA) and images collected by Fluoview FV10i microscope (Olympus, Tokyo, Japan). The number of core protein expressing cells was manually counted in 3-5 randomly selected fields of view.

Southern blot analysis of HBV-DNA

To detect protein-free forms of HBV-DNA including cccDNA, a modified Hirt

extraction procedure was used [4]. Intracellular capsid-associated DNA was prepared as described [15]. Viral DNA forms were separated on an agarose gel, transferred onto a nylon membrane, and hybridized with a digoxigenin-labeled HBV-specific probe [13, 15]. DNA signal was detected by DIG Luminescent Detection Kit (Roche).

Western blot analysis

Western blot analysis was performed essentially as described [15]. For HBx detection, HBV-infected cells in a 35-mm dish were lysed with Pierce RIPA buffer (ThermoFisher Scientific) in the presence of protease inhibitor cocktail (Roche) on ice for 10 min. Primary antibodies used in this study include anti-HBx (5F9 from ViroStat, Portland, Maine, USA), anti-HBVcore (in-house hybridoma supernatant 8C9), polyclonal rabbit anti-HBs serum H863 (kindly provided by S. Urban), anti-actin (SIGMA, St. Louis, MO, USA), and rabbit anti-NTCP serum K9 (kindly provided by B. Stieger) [16].

Results

Optimizing the HBV infection system.

Having selected the HepG2-NTCP-K7 clone (Supplementary Fig.1), we sought to optimize the infection protocol and to investigate the role of DMSO and PEG on different steps of the viral life cycle [5, 17]. We analyzed various HBV markers, including cccDNA, through an experiment in which cells were cultured with or without

2.5% DMSO during and after infection (Fig.1A). Interestingly, we observed a significant reduction in cccDNA, HBV-DNA and HBeAg expression following DMSO withdrawal during (0-3 dpi) or after establishment of infection (3-7 dpi), suggesting a role for DMSO to regulate different steps of the viral life cycle. In the absence of DMSO, cccDNA was reduced 5-fold but the most pronounced effect was on intracellular HBV-DNA. Since pgRNA is reverse transcribed into HBV-DNA, we analyzed HBV transcripts by Northern blot (Fig.1B). DMSO treatment resulted in a dose-dependent increase of all HBV-RNAs. With 2.5% DMSO, HBV 3.5-kb RNA (including pgRNA) and 2.4-/2.1-kb subgenomic RNA levels were 10-fold greater than in DMSO-free cultures (Fig.1C). These data suggest that DMSO has a dual effect on viral cccDNA and RNA levels and 2.5% DMSO was selected for future experimentation.

PEG has been reported to enhance HBV infection by facilitating virus attachment to cell surface heparansulfate proteoglycans [2, 3, 17]. To evaluate whether PEG is required for HBV infection of HepG2-NTCP-K7 cells, cells were inoculated with HBV at increasing multiplicity of infection (moi) in the presence of PEG for 1 day or without PEG for 1-3 days before the inoculum was removed (Fig.1D). At 10 dpi, HBeAg secretion over 48h and the frequency of HBV core expressing cells were determined (Fig.1D-E). Infection rates were significantly higher if PEG was added and reached 77% and 84% at moi 1,000 and 3,000 vp/cell, respectively, while the time of exposure had a minimal effect (Fig.1D). The number of HBV-infected cells was determined by intracellular core protein staining and immunofluorescence microscopy or flow cytometry giving comparable numbers (Supplementary Fig.2).

HBeAg expression increased with the frequency of HBV core expressing cells (Fig.1E). HBV internalization in a synchronized uptake assay increased by 1log10 when PEG was added but was still inhibited by the synthetic pre-S1 peptide, Myrcludex-B (MyrB), demonstrating NTCP dependence (Fig.1F). In summary, these data show that PEG enhances HBV infection, however, a high moi is still required. This led us to use PEG at the time of HBV inoculation and to maintain cells in media containing 2.5% DMSO to achieve optimal infection.

HBV infection kinetics.

To determine the kinetics of HBV infection, we analyzed the expression of viral DNA and RNA species and proteins over time. Southern blot analysis detected cccDNA after 24h and a marked increase was found between 1 and 2 dpi (Fig.2A), suggesting that cccDNA formation is an inefficient and slow process. cccDNA increased further until 3 dpi and thereafter remained at a constant level. The identity of cccDNA was confirmed by both T5 exonuclease treatment where non-cccDNA species are digested [13] and restriction enzyme digestion that linearizes cccDNA (Supplementary Fig.3) [18]. High levels of protein-free rcDNA (PF-rcDNA) were detected 12h after infection that further increased by 1 dpi before declining to almost undetectable levels suggesting that PF-rcDNA is the precursor of cccDNA (Fig.2A) [18, 19]. PF-rcDNA was detected again from 12 dpi after substantial amounts of intracellular rcDNA had been produced (Fig.2B), suggesting that it is derived from both incoming and newly synthesized rcDNA.

To quantify cccDNA levels in our infection model, we used two independent methods,

Southern blot and qPCR (Table1). HepG2-NTCP-K7 cells were infected with increasing moi of HBV and harvested at 3 dpi when cccDNA was fully established from incoming virus, whereas rcDNA was barely detectable (Fig.2A-B). cccDNA copies increased with increasing moi, and 8.2-9.6 copies per cell (i.e., 10.7-12.5 copies per infected cell) were formed following inoculation with 1,000 vp/cell (Table1). These data show that HepG2-NTCP-K7 cells support infection of multiple virus particles.

Northern blot analysis showed that viral transcripts corresponding to HBV pgRNA and subgenomic RNAs were detectable from 3 dpi, increased by 6 dpi and remained constant thereafter (Fig.2C). In parallel, the level of capsid-associated intracellular DNA (i.e. rcDNA and replication intermediates that stem from reverse transcription) and extracellular HBV-DNA increased from 3 to 12 dpi (Fig.2B,D). The high levels of rcDNA observed at 1 dpi are mostly likely derived from input virus associating with cell membranes or vesicles. We observed increasing expression of intracellular HBx, core and surface proteins together with secreted HBsAg and HBeAg reaching a plateau between 12 and 15 dpi (Fig.2E-F). These data highlight the accumulation of viral products over time starting with cccDNA (plateau at 3 dpi), viral RNAs (plateau at 6 dpi) to newly produced rcDNA (plateau at 12 dpi) (Fig.2G). Interestingly, expression kinetics of HBx was faster than that of the other viral proteins. This may imply that HBx could serve as an early viral protein being expressed immediately after infection. The accumulation of viral proteins, on the other hand, could either be a consequence of accumulating transcripts or indicates secondary infection events.

cccDNA persistence during long-term HBV infection.

Having shown the HepG2-NTCP infection model supports robust HBV infection, we investigated how cccDNA is maintained and whether it can be amplified during long-term culture. HBV-infected HepG2-NTCP-K7 cells were cultured for up to 45 days in the presence of 2.5% DMSO, which induces cell cycle arrest [20] and prevents cccDNA loss to cell division [21], and harvested at indicated time points (Fig.3A). In parallel, cells were treated with entecavir (ETV) at a 2,000-fold IC₅₀ from 3 dpi to inhibit reverse transcription and formation of new rcDNA. Southern blot analysis revealed that cccDNA levels modestly increased over time. Treating cells with ETV diminished PF-rcDNA and reduced cccDNA levels by 70% and 48% on 39 and 45 dpi, respectively (Fig.3A). Notably, PF-rcDNA accumulated to high levels over time and this was inhibited with ETV, suggesting that rcDNA-containing capsids refill nuclear HBV-DNA to maintain cccDNA levels [9, 18, 19]. However, the conversion of PF-rcDNA to cccDNA was rate-limiting (Fig.3A). To validate these findings, intracellular cccDNA and total HBV-DNA were determined by qPCR and HBeAg secretion by ELISA (Fig.3B-D). cccDNA levels slowly doubled over time in untreated cells, whereas ETV treatment prevented a cccDNA increase (Fig.3B). HBeAg secretion was gradually increasing until 45 dpi, whereas it peaked at 30 dpi and decreased thereafter under ETV treatment (Fig.3C). As shown in Fig.3D, continuous ETV treatment drastically lowered total intracellular HBV-DNA levels, but without effecting cell viability or morphology (Supplementary Fig.4). Quantifying the number of HBV core expressing cells during the infection also showed a 2-fold difference between control and ETV-treatment at 30 dpi (60±4% vs. 30±8%) (Fig.3E),

confirming our cccDNA data. These results demonstrate that HepG2-NTCP-K7 cells support persistent HBV replication, highlight the long-term stability of cccDNA and indicate that low-level cccDNA **amplification** occurs.

HBV transmission via extracellular particles.

Since the frequency of infected cells increased between 10 and 30 dpi from 39 ± 2 to $60 \pm 4\%$ but **slightly** decreased during ETV-treatment (**Fig.3E**), we hypothesized that secondary infection contributed to maintaining persistent infection. High titer HBV **released into the cell culture medium** (1×10^9 copies/ml i.e. per $1-2 \times 10^6$ cells) would allow this (Fig.2D).

Transfer of media from HBV-infected HepG2-NTCP-K7 cells resulted in cccDNA formation and infection of naïve cells, and - as expected - the efficiency of second round of infection was enhanced by addition of PEG (Fig.4A) [22]. To confirm that HBV transmission is mediated by extracellular virions, HepG2-NTCP-K7 cells were seeded on coverslips and infected with HBV (Fig.4B). After 6 days, coverslips were transferred into new wells together with naïve cells. When co-cultured with one (U2) or three (U3) cover slips of infected cells for 16 days, 4.4% and 17% of naïve target cells expressed viral core protein, respectively, (Fig.4B) and had cccDNA and intracellular HBV-DNA established (Fig.4C). Neutralizing anti-HBs serum (Hepatect) or MyrB blocked HBV transmission (Fig.4D), demonstrating extracellular particle transmission. Transmission of extracellular particles was further supported by a transwell experiment that physically separated HBV-infected producer cells from naïve target cells and prevented cell-cell contact dependent transmission but

facilitated the diffusion of extracellular particles (Supplementary Fig.5). These data demonstrate that progeny virus released from infected HepG2-NTCP-K7 cells can infect naïve cells and support *de novo* cccDNA formation in the absence of PEG.

Since we observed infected cell pairs and groups of 3-5 adjacent HBV core expressing cells (Fig.4B), we wondered whether intracellular particles, presumably mature capsids or enveloped virions, were transmitted to neighboring cells via direct cell-to-cell contact. To investigate this, we co-cultured HBV-infected HepG2-NTCP-K7 cells with HepG2-GFP-Rab7 target cells and monitored the frequency of cells co-expressing GFP-Rab7 and core protein (Fig.5A). However, we could not detect any double positive cells. To evaluate potential NTCP-dependent cell-to-cell transmission, an analogous co-culture experiment was performed with naïve HepG2-NTCP-K7 cells expressing GFP-Rab7 in continuous presence of a neutralizing antibody (Fig.5B). In this setting, only very few double positive cells were detected. Importantly, most of them were not in direct contact with HBV-infected cells (Supplementary Fig.6A), indicating insufficient blockage of *de novo* infection by the anti-HBs antiserum rather than direct cell-to-cell transmission (Supplementary Fig.6B). Collectively, these data suggest that extracellular virus rather than direct cell-to-cell transmission contributes to viral persistence in our *in vitro* infection model.

cccDNA is formed via intracellular recycling of HBV genome.

We next investigated the contribution of intracellular recycling pathway by using a L-HBsAg-deficient, but replication-competent overlength HBV genome (HBV1.3L⁻). Since L-HBsAg is required for infectious progeny virus production and secretion, the

usage of HBV1.3L⁻ genome excludes *de novo* infection via extracellular particles. HBV1.3L⁻ genome was delivered via an adenoviral vector (Ad-HBV1.3L⁻) (Fig.6A-B) [23] or integrated into HepG2-NTCP-K7 cells (Fig.6C) requiring nuclear recycling of HBV rcDNA for establishment of cccDNA. As expected, L-HBsAg was only detected in the sample infected with wild-type HBV (HBVwt), whereas rcDNA and replication intermediates were detected in both Ad-HBV1.3L⁻-transduced and HBVwt-infected cells (Fig.6A). Importantly, Ad-mediated delivery as well as integration of an HBV1.3L⁻ genome resulted in PF-rcDNA sensitive and cccDNA resistant to T5 exonuclease treatment (Fig.6B-C). Since cccDNA formation can only result from nuclear import of capsids, this demonstrates that the intracellular recycling pathway of rcDNA-containing capsids is active and is a driver of cccDNA replenishment.

Discussion

Viruses employ multiple strategies to establish and maintain infection, however, our understanding of HBV transmission pathways to establish chronic infection is limited. In this study, we used the HepG2-NTCP-K7 cell clone that supports efficient HBV replication and enabled us to define HBV infection kinetics, to study for the first time cccDNA dynamics and define pathways maintaining the pool of episomal viral DNA. Infection kinetics was remarkably slow requiring 3 days to establish the cccDNA pool and initiate transcription. RNA levels reached a plateau after 6 days, but protein expression and intracellular HBV-DNA replication took more than 12 days to reach a steady-state. We found that the cccDNA pool once established was very stable for

more than a month and that cccDNA was replenished during the course of infection.

In contrast to previous reports [5, 24], our HepG2-NTCP-K7 cells support secondary HBV infection and intracellular recycling pathway that results in a net cccDNA increase. The K7 clone selected showed more stable NTCP expression and higher HBV susceptibility than the parental cell population and other clones derived thereof (Supplementary Fig.1,7).

Since the longevity and size of an HBV cccDNA pool has not been accurately measured [6], we attempted to determine cccDNA half-life by Southern blot analysis, as the gold standard of cccDNA measurement, and cccDNA-selective qPCR following inhibition of viral DNA synthesis in our cell culture model (Fig.3). These analyses revealed a cccDNA half-life of approximate 40 days determined by Southern blot analysis and even longer than 40 days when measured by qPCR. This difference could be due to variation between assays, DNA isolation methods (Hirt DNA for Southern blot vs. total cellular DNA for qPCR), and/or alteration of reference gene amounts and stability during long-term culture. Of note, controlling cell growth during long-term culture (i.e., 2.5% DMSO, optimal cell seeding density, and regular media exchange) is the critical factor allowing stable maintenance and even low-level amplification of cccDNA. Consistently, the same strategy was applied to determine cccDNA longevity *in vivo* in woodchucks and ducks infected with their respective hepatitis B virus relatives and resulted in similar cccDNA half-lives of 33-50 and 35-57 days, respectively [25, 26].

Next, we determined that in average 1.4-9.6 copies of cccDNA per cell, which

corresponds to 5.0-12.5 copies per infected cell (as determined by positive core staining), are formed and that the copy number is mainly defined by the amount of virus in the inoculum (Table1). cccDNA quantification from two independent methods (Southern blot analysis and selective qPCR) provided very similar data and adds confidence in the use of a well-controlled qPCR to enumerate cccDNA levels in clinical material.

It should, however, be noted that cccDNA detection by qPCR is selective and not specific for cccDNA, and that decent selectivity can be only achieved when the amount of non-cccDNA species (i.e., rcDNA) is relatively low (ideally cccDNA:rcDNA $\leq 1:1000$) [13]; otherwise, false-positive signals arise in late PCR cycles and interfere with conclusions. At 3 dpi from which cccDNA copy number was determined (Table1), the ratio of non-cccDNA species to cccDNA was <50 , whereas it reaches $>1,000$ at 15 dpi (data not shown). Selective cccDNA qPCR in samples containing $>1,000$ copies rcDNA per cccDNA requires pretreatment for instance with T5 exonuclease to remove non-cccDNA species [13]. T5 exonuclease treatment, however, results in a $>20\%$ loss of cccDNA when the level of non-cccDNA species is low (data not shown).

Knowing that a stable cccDNA pool requires to be refilled, the question arose as to how cccDNA is replenished during the course of infection. The mechanism of cccDNA replenishment could be explained by: (i) secondary infection via extracellular particles, (ii) direct cell-to-cell transmission, or (iii) intracellular trafficking of mature, HBV rcDNA-containing capsids back to the nucleus resulting in nuclear reimport of newly formed rcDNA.

Several lines of evidence demonstrate transmission via extracellular virus particles in our HepG2-NTCP-K7 cells. Firstly, extracellular media from HBV-infected cells was capable of infecting naïve target cells in an NTCP dependent manner (Fig.4A). Secondly, the co-culture experiment resulted in cccDNA and core protein expression in naïve target cells that was blocked by entry inhibitors (Fig.4B-D). Finally, physically separating HBV-infected cells from naïve target cells using a transwell assay resulted in HBV-infected target cells (Supplementary Fig.5).

In a chimpanzee, HBV spreads through the liver during acute infection concomitant with a rapid rise of serum HBV-DNA [27]. Similarly, in humanized liver chimeric mice, the frequency of HBV-infected human hepatocytes increases rapidly between weeks 3 and 9 post-infection [28]. Recently, *Xia et al.* reported evidence of HBV spread in hepatocyte-like cells (HLC) derived from pluripotent stem cells [24]. *Michailidis et al.* found that NTCP-expressing HepG2 cells support the complete HBV life cycle including virus spread if PEG is continuously added [22]. Although this is consistent with our finding, PEG may mediate cell fusion and thereby deliver HBV proteins [29]. Thus, our observations are in line with previous reports and highlight the importance of a second round *de novo* infection for maintaining persistent HBV infection.

In our cell culture model, no evidence was obtained for a contribution of direct cell-to-cell transmission to cccDNA increase by co-culture experiments with NTCP-positive and –negative HBV-naïve recipient cells (Fig.5. and Supplementary Fig.6A). Nonetheless, our finding cannot completely exclude this possibility *in vivo*. Endogenous factors required for this process may be lost during transformation into

cancer cells (i.e., HepG2), as in the case of NTCP [4]. Alternatively, two-dimensional cell culture does not adequately reflect polarized structure of hepatocytes and its surrounding extracellular milieu, which may be critical to establish contact between the infected and adjacent uninfected cells. Our finding, however, is consistent with the efficacy of anti-HBs antibodies in post-liver transplant setting and vaccine-induced neutralizing antibodies that efficiently prevent HBV infection in contrast to HCV which can spread via cell-to-cell transmission [12] and for which antibody responses efficiently neutralizing the virus in the clinical setting are lacking.

HBV replication begins from cccDNA which as an episomal, nuclear DNA serves as the transcriptional template and permits persistent infection [1]. In duck hepatitis B virus infection, cccDNA can be amplified via recycling of mature capsid to the nucleus and import of the rcDNA contained [8, 9]. Reverse transcriptase inhibitors such as ETV block maturation of rcDNA inside the viral capsid preventing the formation of infectious virions and thus secondary infection, but also inhibiting intracellular capsid recycling and a refill of cccDNA.

To investigate the contribution of an intracellular recycling pathway in our infection model, we delivered a replication-competent HBV1.3L⁻ genome. Lack of the L-HBsAg (also called envelope protein L) excludes formation of infectious virus and thus secondary infection, but still allows formation of mature HBV capsids that cannot be enveloped and thus are prone to recycle to the nucleus [23]. We demonstrated that both transient and stable delivery of HBV1.3L⁻ genomes resulted in cccDNA formation in HepG2-NTCP-K7 cells (Fig.6), which can only be explained

by nuclear reimport of HBV-DNA from newly formed capsids. Notably, PF-rcDNA drastically accumulated during long-term culture following HBV infection and after delivery of the HBV1.3L⁻ genome, whereas cccDNA levels were not increasing accordingly (Fig.3A and Fig.6). In other studies, the extent of cccDNA accumulation observed in HBV was also markedly lower than that observed in duck hepatitis B virus infection [9, 18, 30]. This indicates that the conversion of PF-rcDNA to cccDNA is a rate-limiting step for cccDNA formation, and our HepG2-NTCP-K7 cells would be an ideal model to identify host factor(s) involved in this process. In addition, the data indicate that preventing rcDNA to cccDNA conversion is an interesting target in attempts to eradicate cccDNA.

In summary, we have generated and characterized a HepG2-NTCP cell clone supporting robust HBV infection. Using this model, we showed that our cells support the complete HBV life cycle from particle entry to infectious particle secretion and determined longevity of an HBV cccDNA pool. Our data sheds light on two major routes of cccDNA replenishment utilized by HBV (i.e., *de novo* infection and intracellular capsid recycling). The infection model will allow us to extend our understanding of poorly characterized steps in the HBV life cycle, for instance cccDNA formation and replenishment and virus dissemination, which could eventually be targeted in attempt to eradicate HBV persistence.

Acknowledgements

We are grateful to Stephan Urban for Myrcludex-B and antiserum H863, Bruno

Stieger for rabbit anti-NTCP serum, and Christoph Seeger for HepAD38 cell line. We thank Samuel Jeske, Konstantin Wolf, Antje Malo, and Thomas Michler for their support and constructive discussion.

References

- [1] Seeger C, Mason WS. Molecular biology of hepatitis B virus infection. *Virology* 2015;479-480C:672-686.
- [2] Schulze A, Gripon P, Urban S. Hepatitis B virus infection initiates with a large surface protein-dependent binding to heparan sulfate proteoglycans. *Hepatology* 2007;46:1759-1768.
- [3] Verrier ER, Colpitts CC, Bach C, Heydmann L, Weiss A, Renaud M, et al. A targeted functional RNA interference screen uncovers glypican 5 as an entry factor for hepatitis B and D viruses. *Hepatology* 2016;63:35-48.
- [4] Yan H, Zhong G, Xu G, He W, Jing Z, Gao Z, et al. Sodium taurocholate cotransporting polypeptide is a functional receptor for human hepatitis B and D virus. *eLife* 2012;1:e00049.
- [5] Ni Y, Lempp FA, Mehrle S, Nkongolo S, Kaufman C, Falth M, et al. Hepatitis B and D Viruses Exploit Sodium Taurocholate Co-transporting Polypeptide for Species-Specific Entry into Hepatocytes. *Gastroenterology* 2014;146:1070-1083 e1076.
- [6] Nassal M. HBV cccDNA: viral persistence reservoir and key obstacle for a cure of chronic hepatitis B. *Gut* 2015;64:1972-1984.
- [7] Watanabe T, Sorensen EM, Naito A, Schott M, Kim S, Ahlquist P. Involvement of host cellular multivesicular body functions in hepatitis B virus budding. *Proc Natl Acad Sci U S A* 2007;104:10205-10210.
- [8] Tuttleman JS, Pourcel C, Summers J. Formation of the pool of covalently closed circular viral DNA in hepadnavirus-infected cells. *Cell* 1986;47:451-460.
- [9] Kock J, Rosler C, Zhang JJ, Blum HE, Nassal M, Thoma C. Generation of covalently closed circular DNA of hepatitis B viruses via intracellular recycling is regulated in a virus specific manner. *PLoS Pathog* 2010;6:e1001082.
- [10] Guo F, Zhao Q, Sheraz M, Cheng J, Qi Y, Su Q, et al. HBV core protein allosteric modulators differentially alter cccDNA biosynthesis from de novo infection and intracellular amplification pathways. *PLoS Pathog* 2017;13:e1006658.
- [11] Sattentau Q. Avoiding the void: cell-to-cell spread of human viruses. *Nat Rev Microbiol* 2008;6:815-826.

- [12] Timpe JM, Stamataki Z, Jennings A, Hu K, Farquhar MJ, Harris HJ, et al. Hepatitis C virus cell-cell transmission in hepatoma cells in the presence of neutralizing antibodies. *Hepatology* 2008;47:17-24.
- [13] Xia Y, Stadler D, Ko C, Protzer U. Analyses of HBV cccDNA Quantification and Modification. *Methods Mol Biol* 2017;1540:59-72.
- [14] Liu C, Cai D, Zhang L, Tang W, Yan R, Guo H, et al. Identification of hydrolyzable tannins (punicalagin, punicalin and geraniin) as novel inhibitors of hepatitis B virus covalently closed circular DNA. *Antiviral Res* 2016;134:97-107.
- [15] Ko C, Shin YC, Park WJ, Kim S, Kim J, Ryu WS. Residues Arg703, Asp777, and Arg781 of the RNase H Domain of Hepatitis B Virus Polymerase Are Critical for Viral DNA Synthesis. *J Virol* 2014;88:154-163.
- [16] Appelman MD, Chakraborty A, Protzer U, McKeating JA, van de Graaf SF. N-Glycosylation of the Na⁺-Taurocholate Cotransporting Polypeptide (NTCP) Determines Its Trafficking and Stability and Is Required for Hepatitis B Virus Infection. *PLoS One* 2017;12:e0170419.
- [17] Gripon P, Diot C, Guguen-Guillouzo C. Reproducible high level infection of cultured adult human hepatocytes by hepatitis B virus: effect of polyethylene glycol on adsorption and penetration. *Virology* 1993;192:534-540.
- [18] Guo H, Jiang D, Zhou T, Cuconati A, Block TM, Guo JT. Characterization of the intracellular deproteinized relaxed circular DNA of hepatitis B virus: an intermediate of covalently closed circular DNA formation. *J Virol* 2007;81:12472-12484.
- [19] Gao W, Hu J. Formation of hepatitis B virus covalently closed circular DNA: removal of genome-linked protein. *J Virol* 2007;81:6164-6174.
- [20] Nikolaou N, Green CJ, Gunn PJ, Hodson L, Tomlinson JW. Optimizing human hepatocyte models for metabolic phenotype and function: effects of treatment with dimethyl sulfoxide (DMSO). *Physiological reports* 2016;4.
- [21] Allweiss L, Volz T, Giersch K, Kah J, Raffa G, Petersen J, et al. Proliferation of primary human hepatocytes and prevention of hepatitis B virus reinfection efficiently deplete nuclear cccDNA in vivo. *Gut* 2017.
- [22] Michailidis E, Pabon J, Xiang K, Park P, Ramanan V, Hoffmann HH, et al. A robust cell culture system supporting the complete life cycle of hepatitis B virus. *Sci Rep* 2017;7:16616.
- [23] Sprinzl MF, Oberwinkler H, Schaller H, Protzer U. Transfer of hepatitis B virus genome by adenovirus vectors into cultured cells and mice: crossing the species barrier. *J Virol* 2001;75:5108-5118.
- [24] Xia Y, Carpentier A, Cheng X, Block PD, Zhao Y, Zhang Z, et al. Human stem cell-derived hepatocytes as a model for hepatitis B virus infection, spreading and virus-host interactions. *J Hepatol* 2017;66:494-503.

- [25] Zhu Y, Yamamoto T, Cullen J, Saputelli J, Aldrich CE, Miller DS, et al. Kinetics of hepadnavirus loss from the liver during inhibition of viral DNA synthesis. *J Virol* 2001;75:311-322.
- [26] Addison WR, Walters KA, Wong WW, Wilson JS, Madej D, Jewell LD, et al. Half-life of the duck hepatitis B virus covalently closed circular DNA pool in vivo following inhibition of viral replication. *J Virol* 2002;76:6356-6363.
- [27] Thimme R, Wieland S, Steiger C, Ghrayeb J, Reimann KA, Purcell RH, et al. CD8(+) T cells mediate viral clearance and disease pathogenesis during acute hepatitis B virus infection. *J Virol* 2003;77:68-76.
- [28] Volz T, Allweiss L, Ben MM, Warlich M, Lohse AW, Pollok JM, et al. The entry inhibitor Myrcludex-B efficiently blocks intrahepatic virus spreading in humanized mice previously infected with hepatitis B virus. *J Hepatol* 2013;58:861-867.
- [29] Lempp FA, Mutz P, Lipps C, Wirth D, Bartenschlager R, Urban S. Evidence that hepatitis B virus replication in mouse cells is limited by the lack of a host cell dependency factor. *J Hepatol* 2016;64:556-564.
- [30] Summers J, Smith PM, Huang MJ, Yu MS. Morphogenetic and regulatory effects of mutations in the envelope proteins of an avian hepadnavirus. *J Virol* 1991;65:1310-1317.

Tables

Table1. cccDNA copy number in HBV-infected HepG2-NTCP-K7 cells

Multiplicity of infection	Southern blot ^a		qPCR ^b	
	per cell	per infected cell	per cell	per infected cell
100 vp/cell	2.5 ± 1.0	9.2 ± 3.8	1.4 ± 0.6	5.0 ± 2.3
300 vp/cell	5.3 ± 0.9	9.9 ± 1.8	3.0 ± 1.2	5.7 ± 2.2
1000 vp/cell	9.6 ± 0.9	12.5 ± 1.2	8.2 ± 2.1	10.7 ± 2.7

Note. HBV-infected HepG2-NTCP-K7 cells were harvested at 3 dpi for DNA extraction and subjected to cccDNA copy number determination. Prior to DNA extraction, cells were trypsinized and counted. The number of infected cells was determined by counting core protein-positive cells (Fig. 1D). Mean±SD is given.

^aProtein-free DNAs extracted by modified Hirt method were subjected to Southern blot analysis. Standard curves were generated by preparing serial dilution of a 3.2-kb double-stranded linear HBV genome. The experiment was performed twice.

^bTotal cellular DNA was subjected to cccDNA-selective qPCR without prior T5 exonuclease treatment. Standard curves were generated by preparing serial dilution of a plasmid DNA containing HBV monomer for qPCR. The experiment was repeated three times.

Figure legends

Fig.1. Role of DMSO and PEG in HepG2-NTCP infection model. (A) HepG2-NTCP-K7 cells were infected with HBV and maintained with or without 2.5% DMSO from the time of infection as indicated. Viral DNA and HBeAg levels were measured by qPCR and ELISA, respectively. (B) Cells were cultured with increasing concentrations of DMSO (up to 3.5%) one day after HBV infection. Total RNA was extracted at 7 dpi and subjected to Northern blot analysis using an HBV-DNA probe. Viral RNA was quantified with 2.5% DMSO condition set to 100%. Ribosomal RNA (28S and 18S) stained by ethidium bromide is shown as a loading control. (C) The amount of total RNA from a 35-mm dish extracted at respective conditions (black line with solid circle) and the relative amount of HBV-RNA normalized to total RNA (gray bar) are given. (D, E) HepG2-NTCP-K7 cells were infected with either increasing moi (100, 300, 1000, and 3000 vp/cell) of HBV in the absence of PEG or at an moi of 100 vp/cell in the presence of PEG for 1, 2 and 3 days as indicated. (D) Cells were fixed and stained for HBV core protein and the **percentage** of infected cells is denoted at the bottom-right corner of each image. (E) HBeAg was determined in extracellular media. (F) HBV uptake was determined with or without PEG in the presence or absence of an entry inhibitor Myrcludex-B (MyrB). HBV genomes inside the cells were quantified by qPCR. Statistical significance was determined using Student's t test (*p <0.05, **p <0.01, ***p <0.001). dpi: day post-infection. moi: multiplicity of infection. vp: virus particle.

Fig.2. Kinetics of the HBV-DNA forms, viral RNA, and protein expression in

HepG2-NTCP-K7 cells

(A-F) HepG2-NTCP-K7 cells were infected with HBV at an moi of 1,000 vp/cell. At indicated time points, (A) DNA extracted after Hirt lysis and (B) intracellular capsid-associated DNA, and (C) total RNA were detected by Southern or Northern blot analysis, respectively using an HBV-DNA probe. (D) Extracellular HBV-DNA was quantified by qPCR. (E) Intracellular HBx, core, and surface proteins were detected by Western blot analysis. (F) Secreted HBsAg and HBeAg were quantified by immunoassay. (G) Each band or value determined at different time points in panel A to F was quantified and plotted. Values from 15 dpi were set to 100%.

Fig.3. Dynamics of cccDNA during long-term culture of HBV-infected HepG2-NTCP-K7 cells

(A-D) HepG2-NTCP-K7 cells were infected with HBV at an moi of 300 vp/cell (A) or 100 vp/cell (B-D) and kept with or without ETV (1 μ M) treatment from 3 dpi onwards. (A) DNA was isolated after Hirt extraction at different time points and subjected to Southern blot analysis using an HBV-DNA probe. Restriction fragments of HBV-DNA (3.2 kb to 1.4 kb; open arrowheads) on first and last lanes serve as size marker and as efficiency control of Southern blot transfer. Percent values below each lane indicate the relative amount of cccDNA. (B-D) cccDNA and total intracellular HBV-DNA, and HBeAg levels were measured by qPCR and ELISA, respectively. For cccDNA measurement, both absolute copy numbers and relative cccDNA values to *PRNP* and *MT-CO3* are given. (E) Cells were infected with HBV at an moi of 300 vp/cell and treated with ETV from 3 dpi. Intracellular HBV core protein was visualized

by immunofluorescence staining at 10, 20, and 30 dpi. The number of core protein-positive cells at each time point was counted and is plotted in a bar graph. Statistical significance was determined using Student's t test (**p <0.01).

Fig.4. Analysis of *de novo* infection mediated by extracellular virions

(A) Cell-culture media from HBV-infected HepG2-NTCP-K7 cells were transferred onto naïve cells with or without PEG. At 11 days post-transfer, cccDNA and total intracellular HBV-DNA were analyzed by qPCR. (B) For co-culture experiment in a physically separated setting, HepG2-NTCP-K7 cells were seeded on cover-slips and either treated with PEG only or infected with HBV at an moi of 1,000 vp/cell with PEG. At 6 dpi, cover-slips with infected cells were transferred into new wells together with cover-slips with non-infected cells as depicted and subsequently co-cultured for 16 days in the absence of PEG. Naïve target cells from each condition (denoted U1, U2 and U3) were subjected to immunofluorescence staining with an anti-core antibody. (C) cccDNA and total intracellular HBV-DNA contents were analyzed by qPCR. Target cells were treated with trypsin for 5 min to remove cell surface bound HBV prior to DNA isolation. (D) The same experiment performed (condition U2) in the presence or absence of entry inhibitors (0.5 IU/ml Hepatect CP or 200 nM MyrB). The percentage of infected cells is denoted at the bottom-right corner of each image.

Fig.5 Evaluation of cell-to-cell transmission of HBV. (A) HepG2-GFP-Rab7 cells and HBV-infected HepG2-NTCP-K7 cells were co-seeded into a 24-well plate at three different ratios and co-cultured. (B) HepG2-NTCP-K7-GFP-Rab7 cells and HBV-infected HepG2-NTCP-K7 cells were co-cultured at three different ratios in the

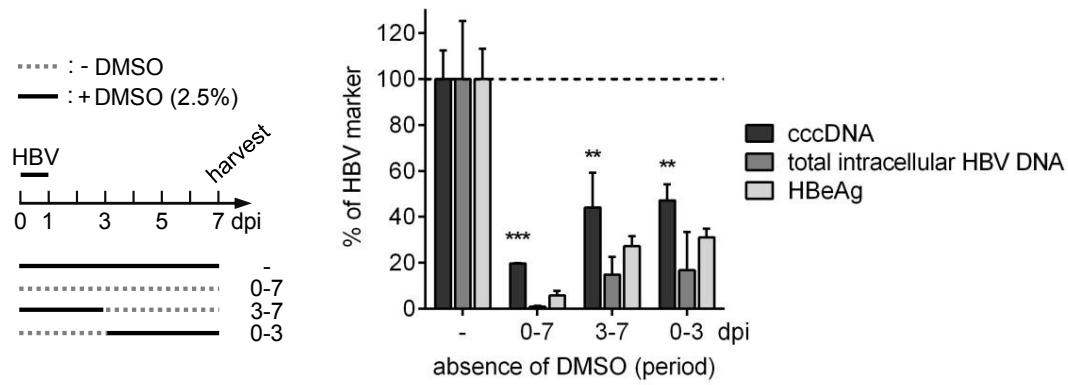
continuous presence of neutralizing antibodies (NAb; 0.5 IU/ml Hepatect CP). After 21 days, cells were fixed, stained with an anti-core antibody, and analyzed by immunofluorescence staining. GFP signal was visualized in parallel.

Fig.6. Nuclear recycling of HBV1.3L- genomes

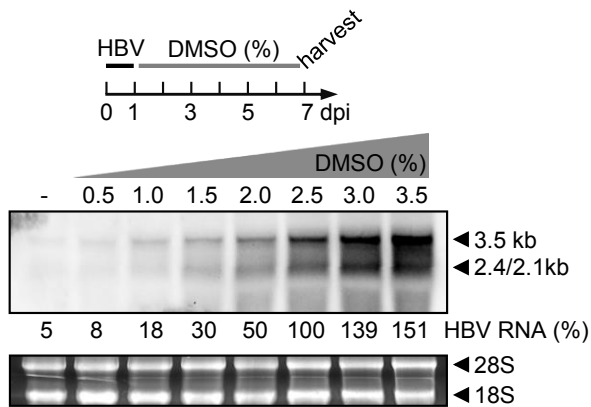
(A, B) HepG2-NTCP-K7 cells were either transduced with Ad-HBV1.3L⁻ or Ad-Ctrl at an moi of 20 infectious units (IU)/cell or infected with HBV at an moi of 500 vp/cell. (A) Intracellular capsid-associated HBV-DNA was analyzed by Southern blotting at day 11. An aliquot of cell lysate prepared during the HBV-DNA isolation was subjected to Western blot analysis using an anti-HBsAg serum. β -actin served as a loading control. (B) DNA extracted after Hirt lysis was assayed by Southern blot following T5 exonuclease digestion, if indicated. (C) HepG2-NTCP-K7-H1.3L⁻ cells were cultured and harvested at the indicated time points and Hirt-extracted DNA was analyzed by Southern blotting. Identity of cccDNA was confirmed by T5 exonuclease digestion.

Figure 1. Role of DMSO and PEG in HepG2-NTCP infection model

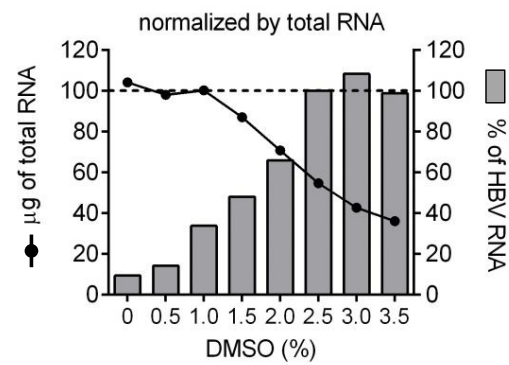
A



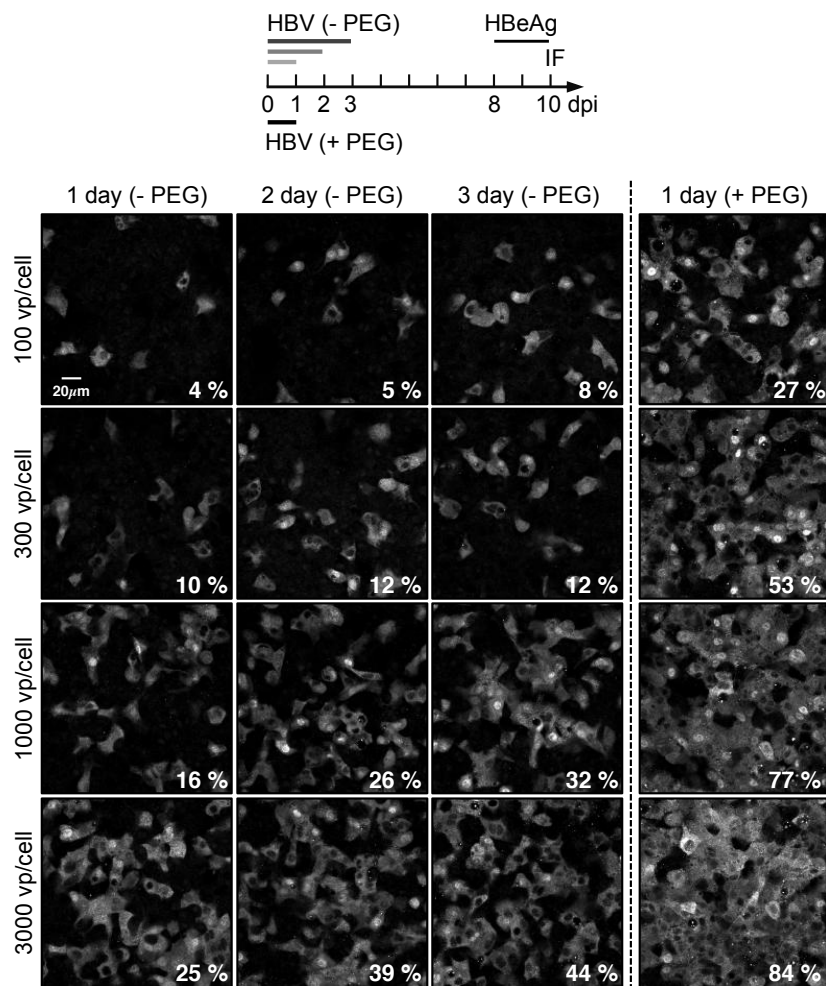
B



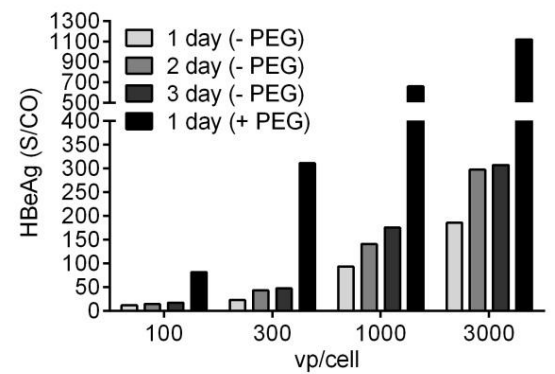
C



D



E



F

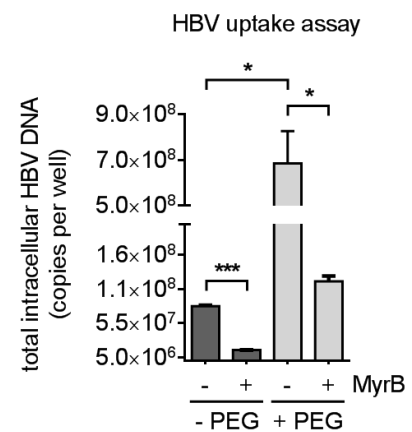


Fig. 2. Kinetics of the HBV DNA forms, viral RNA, and protein expression in HepG2-NTCP-K7 cells

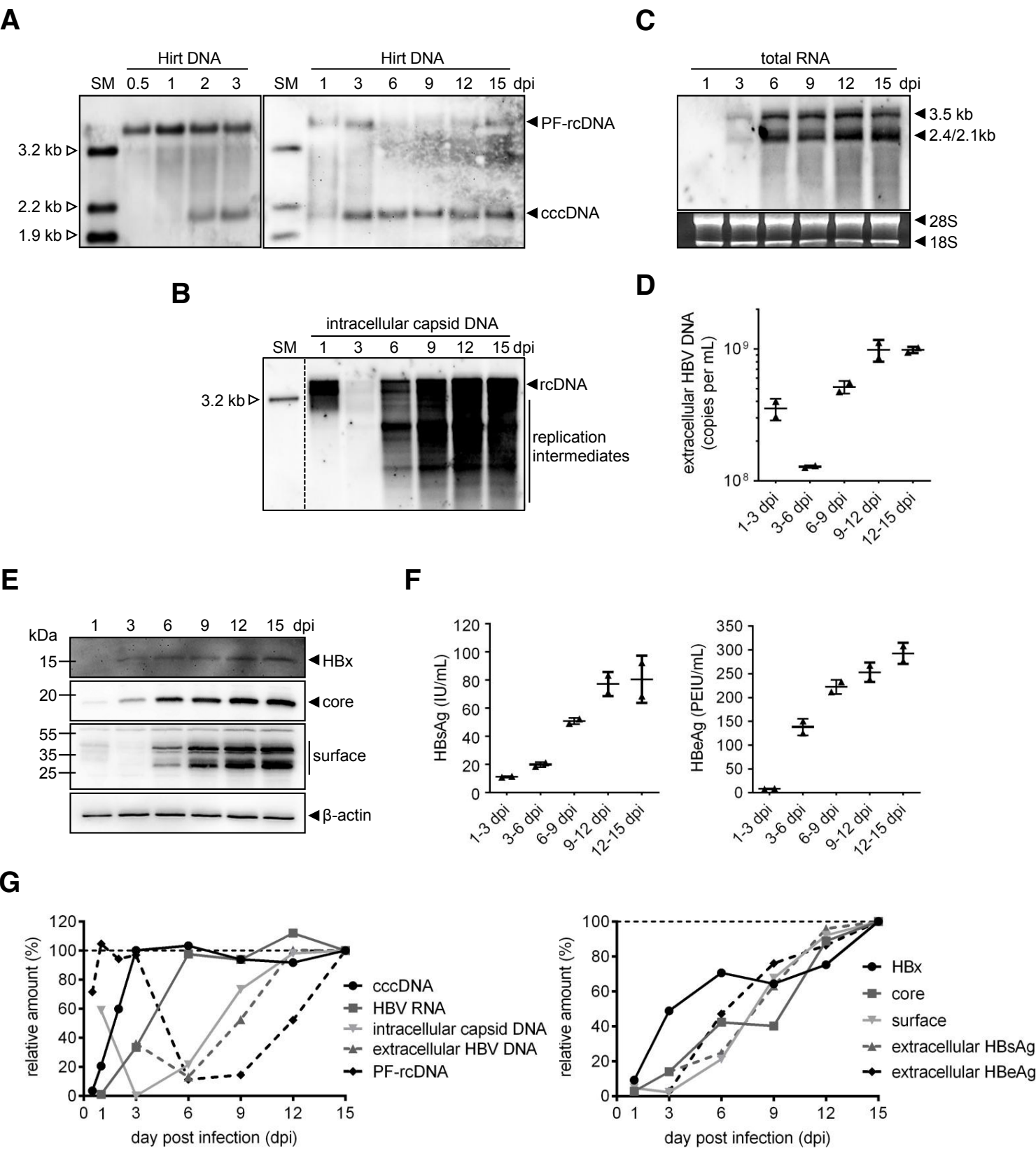


Fig. 3. Dynamics of cccDNA during long-term culture of HBV-infected HepG2-NTCP-K7 cells

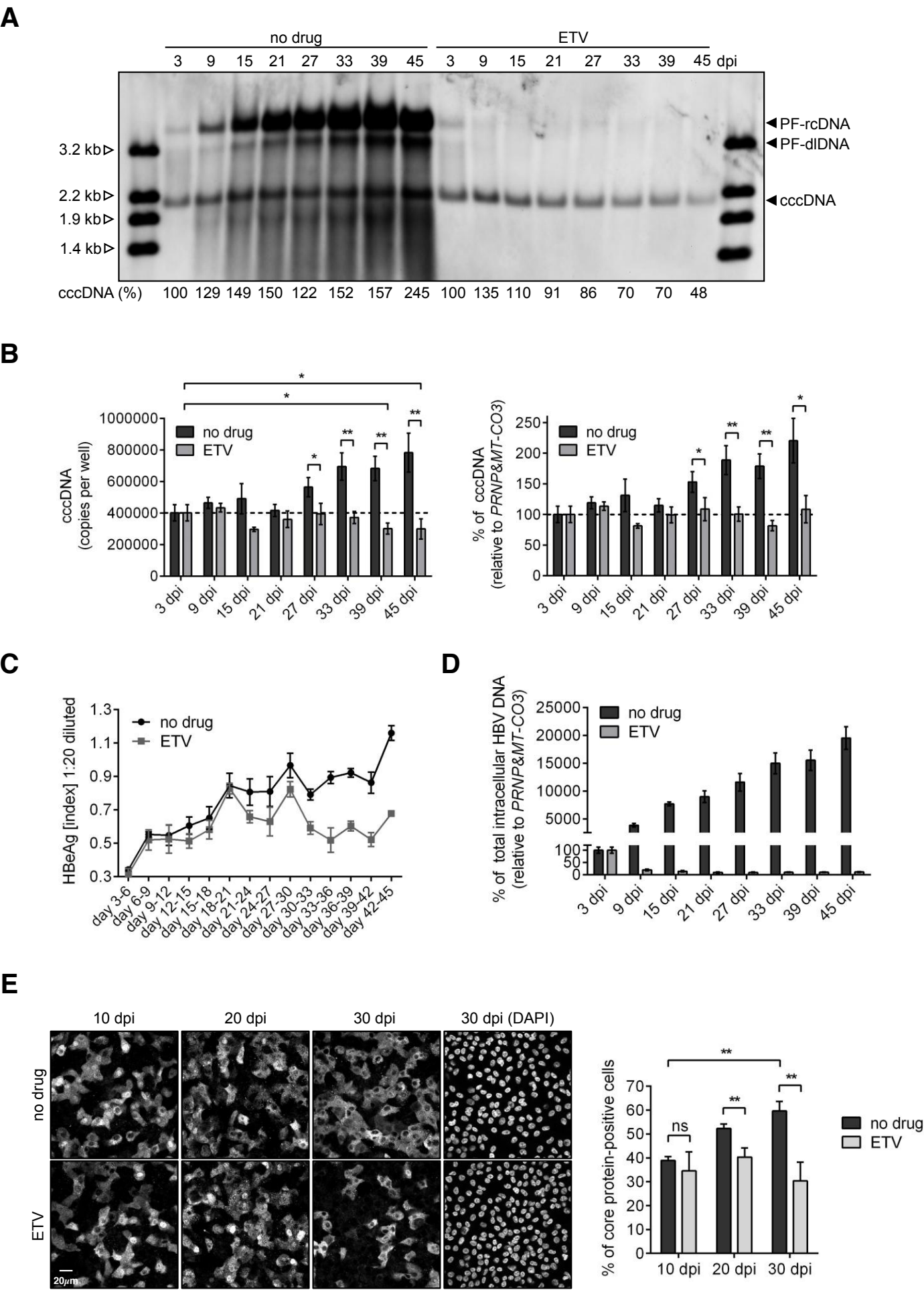


Fig. 4. Analysis of *de novo* infection mediated by extracellular virions

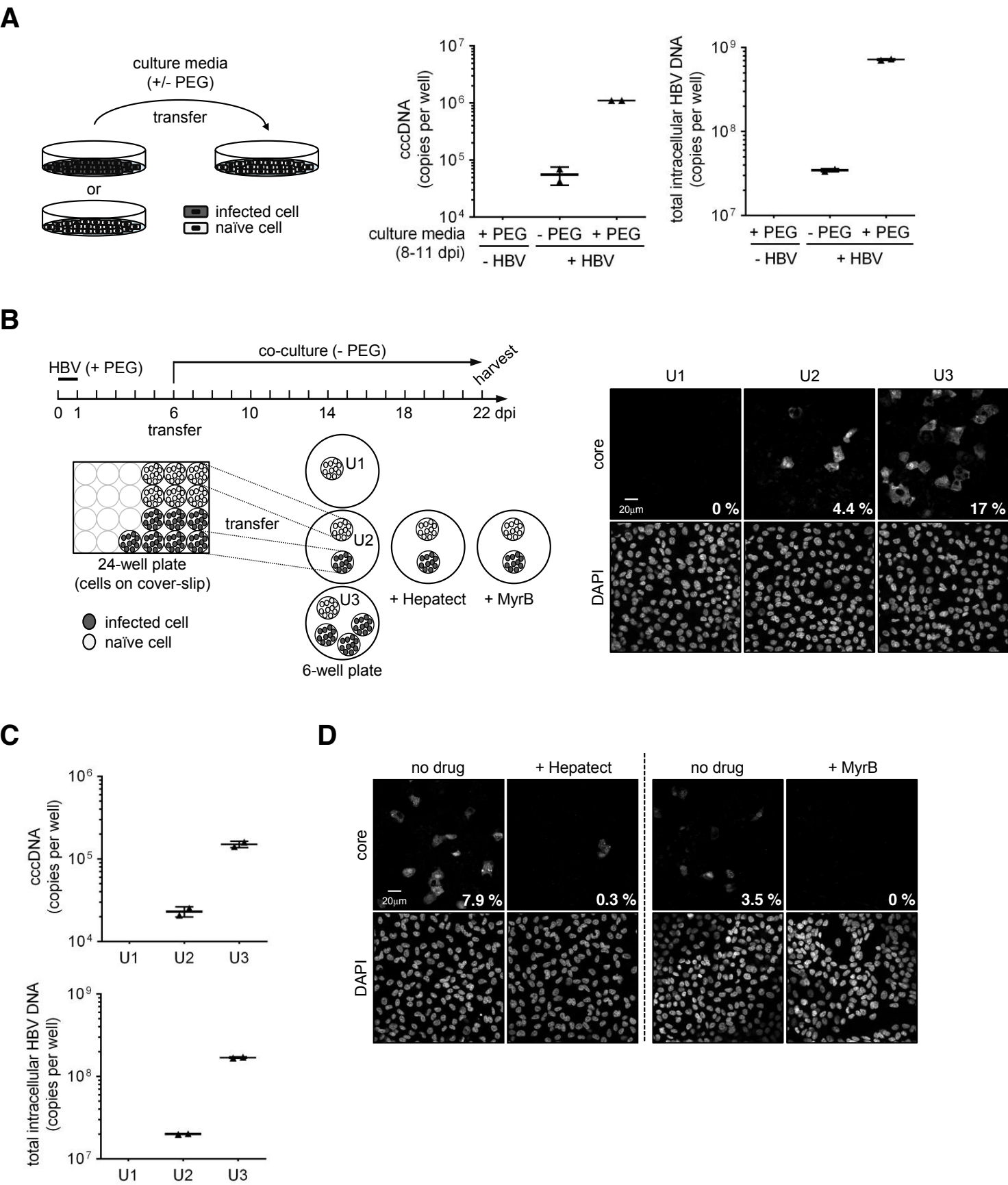
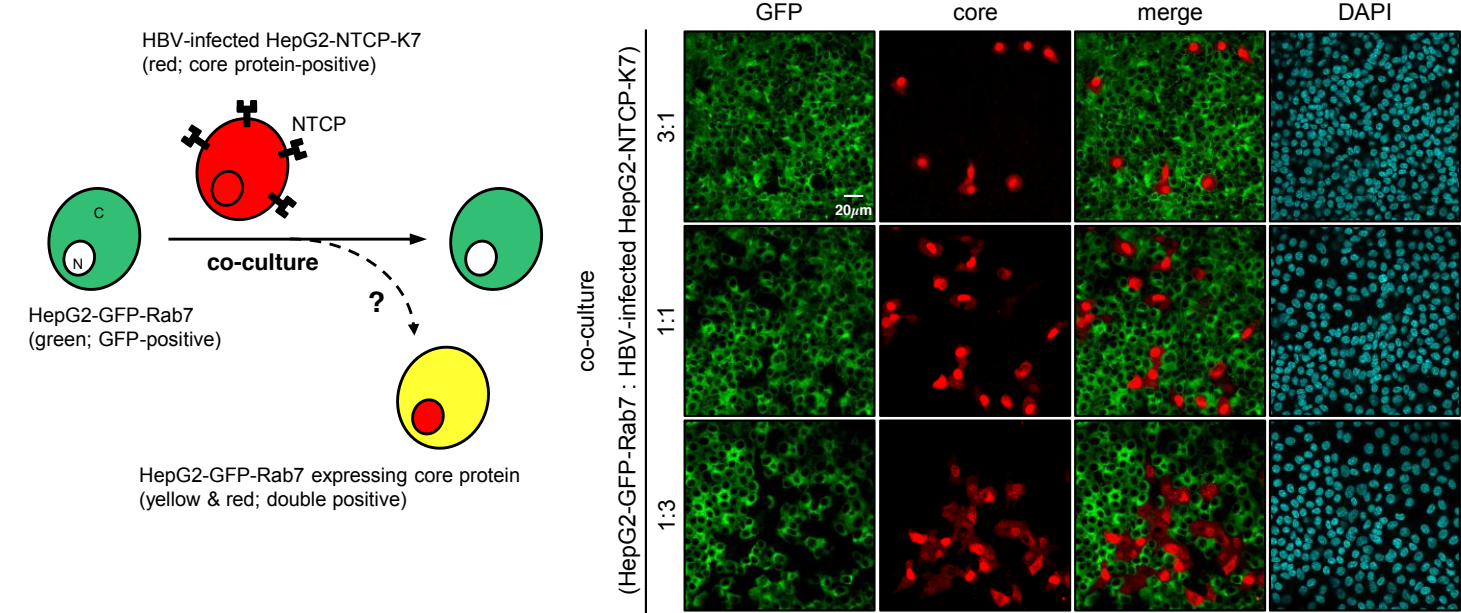


Fig. 5. Evaluation of cell-to-cell transmission of HBV

A



B

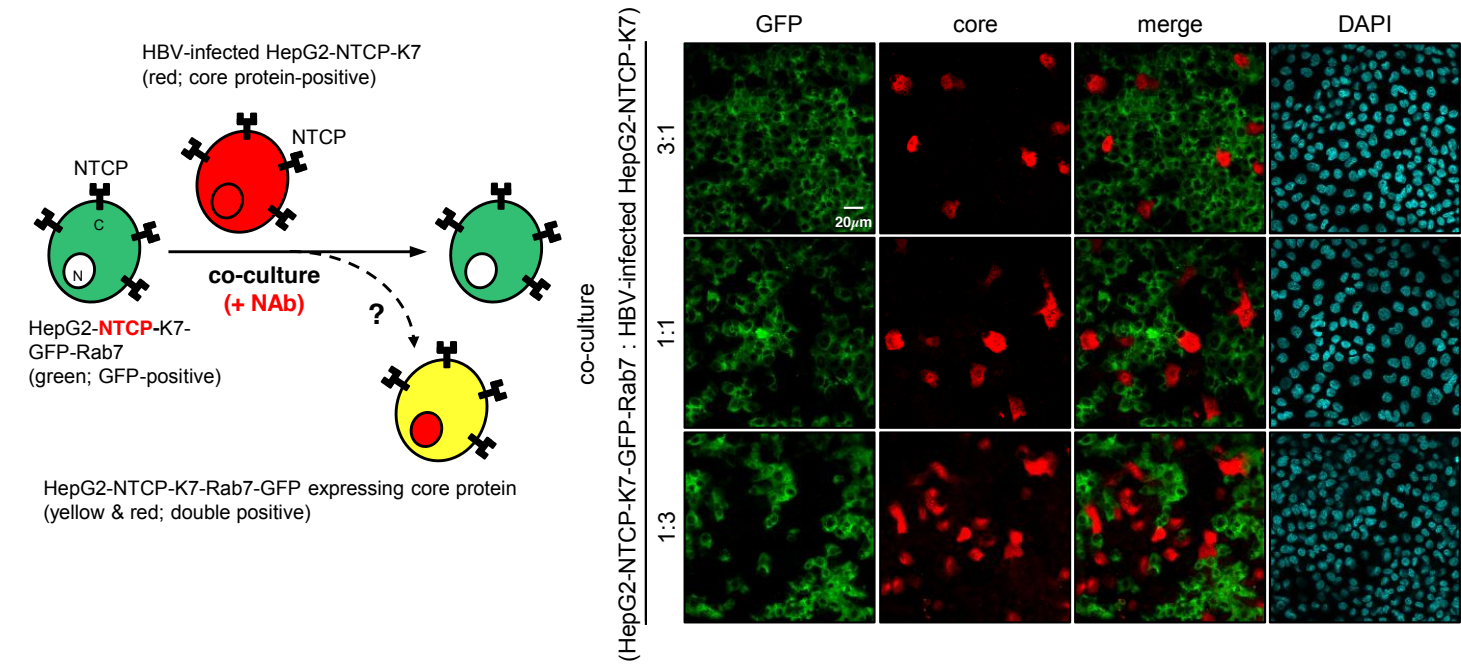
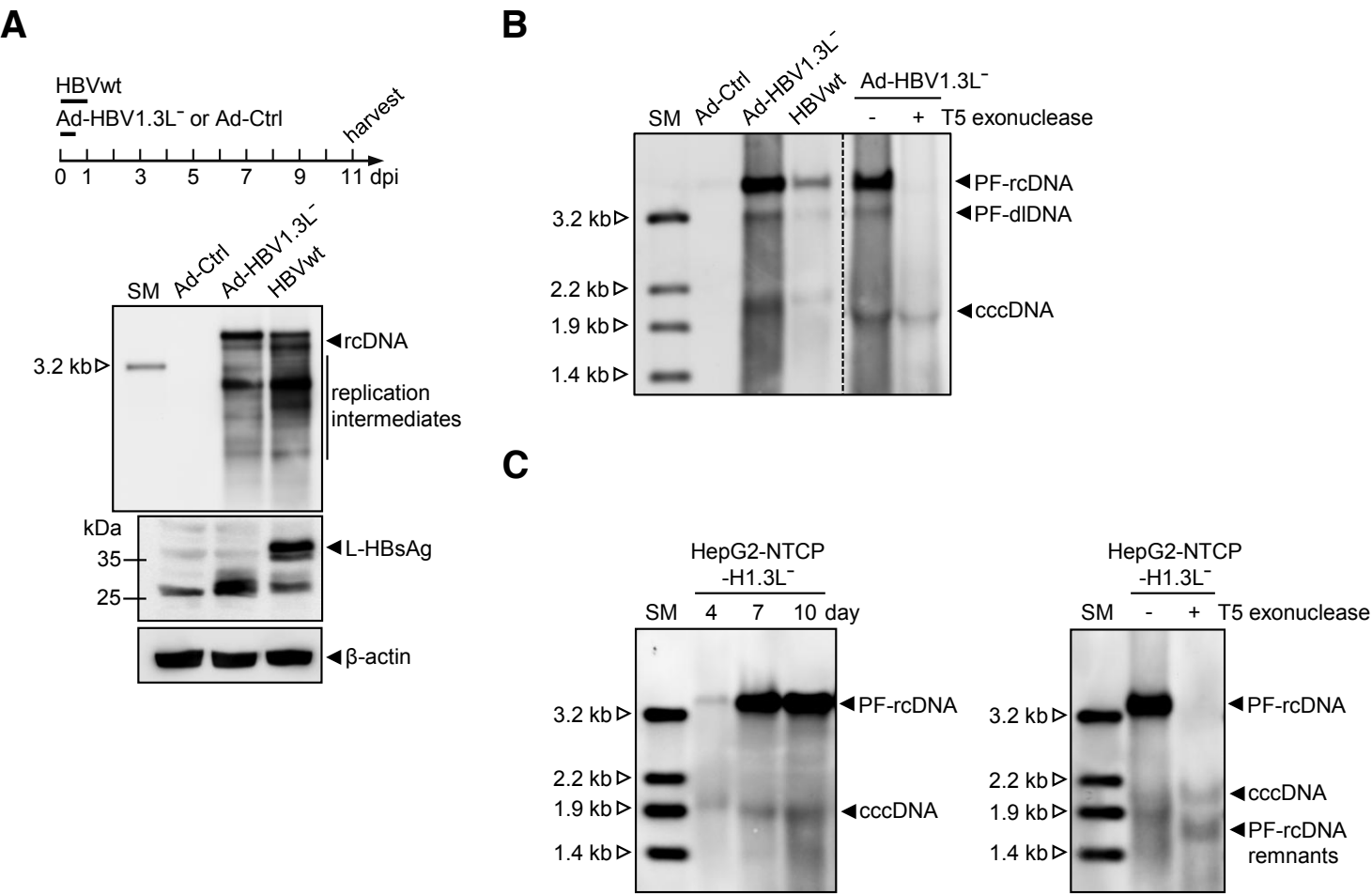
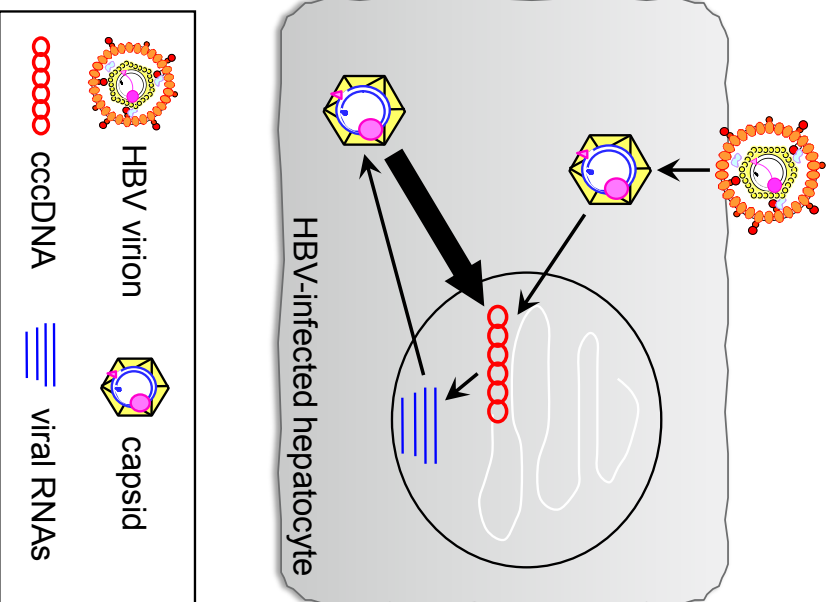


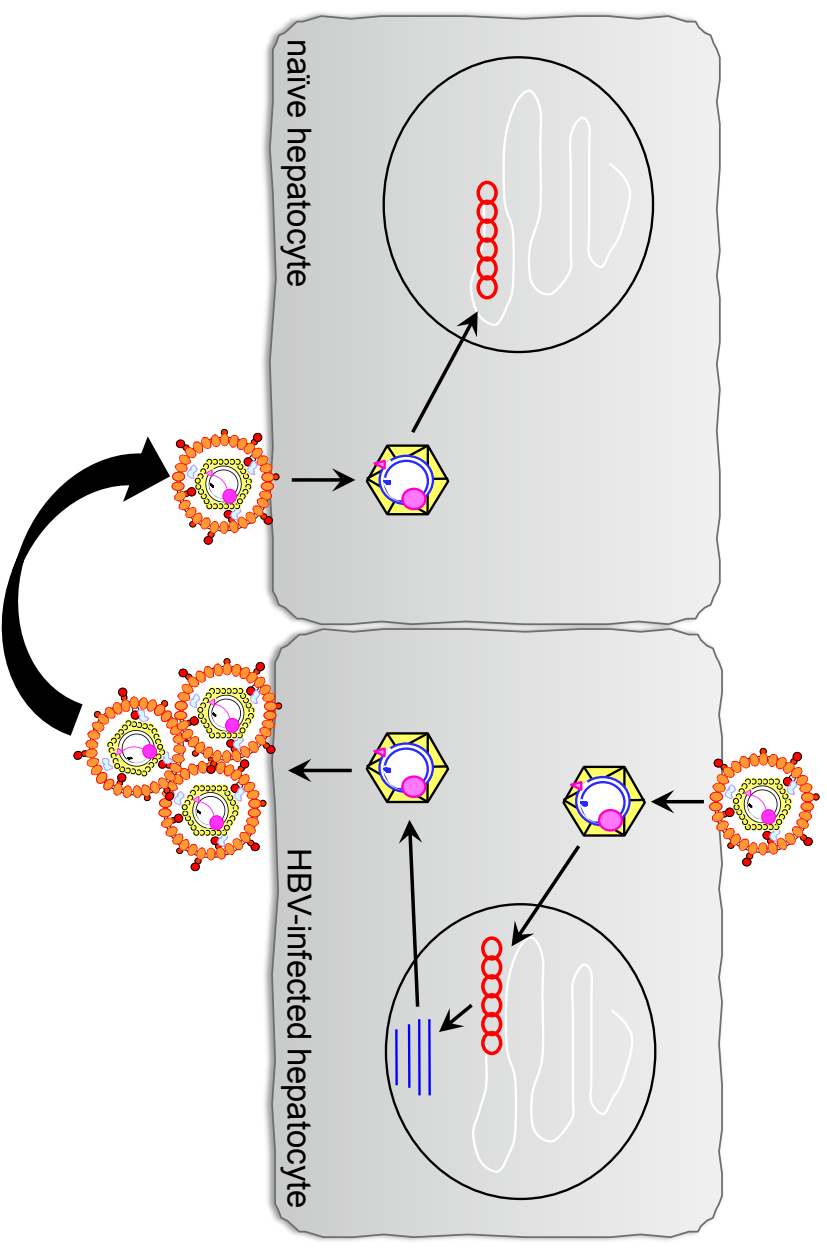
Fig. 6. Nuclear recycling of HBV1.3L⁻ genomes



1. intracellular capsid recycling



2. *de novo* secondary infection



Highlights

- Studying HBV has been limited by the availability of *in vitro* and *in vivo* models.
- A selected HepG2 cell clone expressing NTCP supports long-term HBV infection.
- HBV has a slow infection kinetics requiring 3 days for full establishment of infection.
- 1-9 copies of cccDNA per cell are established with an estimated half-life of 40 days.
- cccDNA levels remain stable by intracellular capsid recycling and secondary infection.

Supplementary material

[Click here to download Supplementary material: K7_Suppl_revision_final_marked.docx](#)

***ICMJE disclosure form**

[Click here to download ICMJE disclosure form: K7_disclosure forms_final.pdf](#)